Supporting Information

Akondy et al. 10.1073/pnas.1500475112

SI Methods

Analysis of Activated T Cells by Flow Cytometry. Two separate lots of the vaccine were used, with the first 64 participants receiving lot UE804AA and the remaining 16 receiving lot UE984AA. Blood was drawn at various days postvaccination such that it did not exceed 250 mL in a 6-wk period. PBMC were purified from cell preparation tubes (BD Biosciences) using standard protocols. All vaccinees had seroconverted by day 14 as seen in plaque reduction neutralizing antibody assays.

The magnitude of the YFV-specific response was measured in whole blood using activation markers or using tetramers recognizing CD8 T cells specific for the HLA-A2 restricted $NS4B^{214}$ epitope. T cells activated in the course of an acute infection undergo rapid proliferation and down-regulate the antiapoptotic protein Bcl-2. This expanding population can be identified using binding to the Ki-67 antigen, expression of which is tightly coupled to cell cycle. Thus, the $Ki\text{-}67^{+}Bcl\text{-}2^{lo}$ phenotype occurs transiently during the expansion stage and can be measured by flowcytometric analysis. Because the volunteers in this study were healthy and had no ongoing infections at the time of vaccination, prevaccination frequencies of the activated T cells were very low (<0.5% for CD8 T cells), and an increase in their frequency can be used as an estimate of the magnitude of the total, virus-elicited CD4 or CD8 T-cell response (1). For brevity we refer to $Ki\text{-}67^{+}Bcl\text{-}2^{lo}$ CD8 T cells as $Ki\text{-}67^{+}$ CD8 T cells in the text. In a subset of individuals that were HLA-A2 positive we used tetramers to identify CD8 T cells specific for the HLA-A2 restricted NS4B 214–222 epitope of YFV. All antibodies used in this study were obtained from BD Biosciences, and $A2\text{-}NS4B^{214}$ tetramers were made in house. Staining of samples, data acquisition, and analysis were done as described previously (2).

Measurement of YFV-17D Viral Genomes in Blood. Plasma isolated from blood samples was used to assay YFV-17D genomes using a TaqMan real-time PCR (Applied Biosystems). The following primers were used: 5′-CTACGTGTCTGGAGCCCGCAGCAAT-3′ (FAM- and TAMRA-labeled TaqMan probe), 5′-GAACAGTGATCAGGAACCCTCTCT-3′ (Forward primer), and 5′-GGATGTTTGGTTCACAGTAAATGTG-3′ (Reverse primer). Primers for real-time PCR were designed within the highly conserved NS5 gene of YFV with Primer Express software (Applied Biosystems). RNA was isolated from plasma samples with a QIAamp viral RNA minikit (QIAGEN). The two-step reverse transcriptase (RT)-PCR was performed with a TaqMan Gold kit under the following conditions: The 50-µL reactions contained 5 µL of 10× TaqMan buffer A, 4 mM MgCl2, 400 µM dNTPs, a 200 nM concentration of each primer, a 12 nM concentration of the fluorogenic probe, 2.5 µM of random hexamers, 1.25 units of AmpliTaq Gold DNA polymerase (Applied Biosystems), 20 units of recombinant Mo-MuLVMultiScribe, and 8 units of RNase inhibitor in 20 µL volume for reverse transcription. Thermal cycling conditions consisted of 10 min at 25 °C, 20 min at 42 °C, 5 min at 99 °C (first step), 10 min at 95 °C, and then 45 cycles of 15 s at 95 °C and 1 min at 60 °C. Absolute quantification of RNA transcripts was determined with RNA template standards and to estimate the detection threshold (21 genomes per mL).

Analysis of Early Gene Expression Signatures. Gene expression signatures before and various days postvaccination were obtained for 14 of the 80 vaccinated donors. In brief, total RNA from fresh PBMCs of vaccinees was purified, labeled, and hybridized on Human U133 Plus 2.0 Arrays as described earlier (ref. 3 and GSE13486). The microarray intensity data of probe sets were normalized by RMA. Probe sets representing the same gene were collapsed by taking the probe set with highest absolute mean $\log_2$ fold-change among all day 3 versus day 0 and day 7 versus day 0 values. Pearson correlation ($R > 0.4$ or < -0.4 and P value < 0.01) was used to identify genes whose expression at baseline and days 3 and 7 postvaccination correlated with viral load measured at the same time points. Ingenuity pathway analysis was used to identify networks that were enriched in the differentially expressed genes. GSEA (3) was performed to determine whether the rank-ordered list of viral load correlated genes (i.e., genes ranked by their Pearson correlation values) was enriched in genes associated with type I IFN (4) and T-cell memory signatures (GSE11057, GSE23321, and E-TABM-40). The parameters used in the GSEA were the weighted enrichment statistic with 1,000 permutations.

1. Miller JD, et al. (2008) Human effector and memory CD8+ T cell responses to smallpox and yellow fever vaccines. *Immunity* 28(5):710–722.
2. Akondy RS, et al. (2009) The yellow fever virus vaccine induces a broad and polyfunctional human memory CD8+ T cell response. *J Immunol* 183(12):7919–7930.
3. Querec TD, et al. (2009) Systems biology approach predicts immunogenicity of the yellow fever vaccine in humans. *Nat Immunol* 10(1):116–125.
4. Subramanian A, et al. (2005) Gene set enrichment analysis: A knowledge-based approach for interpreting genome-wide expression profiles. *Proc Natl Acad Sci USA* 102(43):15545–15550.
5. Schoggins JW, et al. (2011) A diverse range of gene products are effectors of the type I interferon antiviral response. *Nature* 472(7344):481–485.

Fig. S1. Viral load and CD8 response in HLA-A2$^+$ individuals. For each HLA-A2$^+$ individual, subplots show kinetics of viral titer (red) and YFV-specific CD8 cells measured by Ki-67$^+$Bcl-2^{lo} phenotype (dashed blue) and by the NS4B^{214} tetramers (green). Tetramer$^+$ CD8 T cells peak after Ki-67. This is because the total number of YFV-specific cells continues to rise when there is limited proliferation measured by Ki-67 even if the latter is past its maximum level.

Fig. S2. Relationship between the time of the peak viral load and its magnitude, as well as the magnitude of the CD8 T-cell response. (*A*) Individuals that peaked earlier (day 5) have a slight but significantly higher peak virus load than those that peak later (day 7). (*B*) The mean effector CD8 (% Ki-67$^+$Bcl-2^{lo}) shows no significant difference between those individuals with viral peaks at day 5 (solid black line) vs. day 7 (dashed blue line). Error bars indicate SEM.

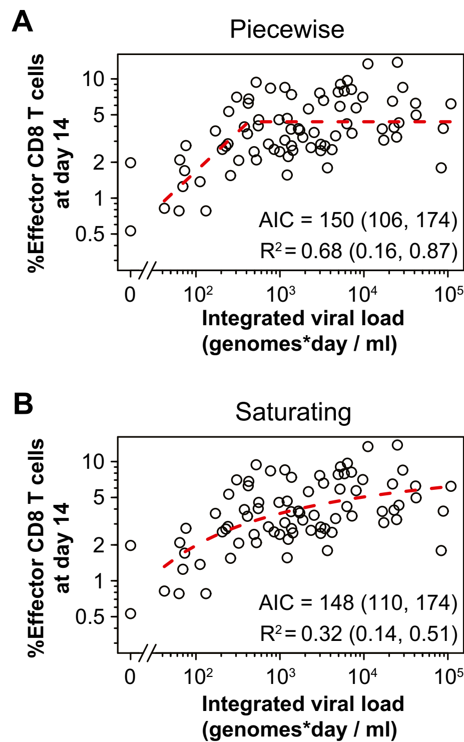

Fig. S3. Correlation between viral load and CD8 effector response is robust. Fig. 4 *B* and *C* show a strong correlation between peak viral load and the CD8 effector response. Here we show that a similar result holds if we use integrated viral load in the place of peak viral load. *A* shows the fit to a piecewise-linear model, and *B* shows the fit to a smooth saturating model for the relationship between CD8 response and integrated viral load. The R^2 value for the piecewise model is for the data before saturation. The AIC values and their ranges obtained by bootstrap show that both models describe the data comparably well.

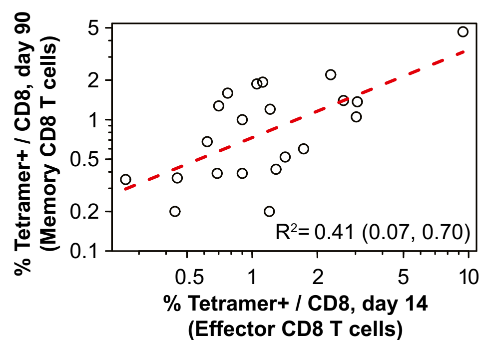

Fig. S4. Magnitude of a CD8 tetramer-specific effector response is correlated with the magnitude of the corresponding memory response. Although the Ki-67^+Bcl-2^{lo} marker can only be used at an effector time point, tetramers can be used at both effector and memory time points. We plot frequencies of the $NS4B^{214}$ tetramer at effector (day 14) and memory (day 90) stages for the subset of donors who were HLA-$A2^+$. Linear regression of these quantities yielded an R^2 = 0.41 with a 95% confidence interval of 0.07–0.70.